

File ID uvapub:3765
Filename 2300431.pdf
Version unknown

SOURCE (OR PART OF THE FOLLOWING SOURCE):

Type article
Title The 1998 outburst of the X-ray transient 4U 1630-47 observed with
 BeppoSAX
Author(s) T. Oosterbroek, A.N. Parmar, E. Kuulkers, T. Belloni, M. van der Klis, F.
 Frontera, A. Santangelo
Faculty FNWI: Astronomical Institute Anton Pannekoek (IAP)
Year 1998

FULL BIBLIOGRAPHIC DETAILS:

<http://hdl.handle.net/11245/1.140494>

Copyright

It is not permitted to download or to forward/distribute the text or part of it without the consent of the author(s) and/or copyright holder(s), other than for strictly personal, individual use, unless the work is under an open content licence (like Creative Commons).

The 1998 outburst of the X-ray transient 4U 1630–47 observed with *BeppoSAX*

T. Oosterbroek¹, A.N. Parmar¹, E. Kuulkers², T. Belloni³, M. van der Klis³, F. Frontera⁴, and A. Santangelo⁵

¹ Astrophysics Division, Space Science Department of ESA, ESTEC, P.O. Box 299, 2200 AG Noordwijk, The Netherlands

² Astrophysics, University of Oxford, Nuclear and Astrophysics Laboratory, Keble Road, Oxford OX1 3RH, UK

³ Astronomical Institute, University of Amsterdam and Center for High-Energy Astrophysics, Kruislaan 403, 1098 SJ Amsterdam, The Netherlands

⁴ Istituto TESRE, CNR, via Gobetti 101, I-40129 Bologna, Italy

⁵ IFCAI, CNR, via La Malfa 153, I-90146 Palermo, Italy

Received 10 August 1998 / Accepted 30 September 1998

Abstract. We report results of five pointed *BeppoSAX* observations of the black hole candidate 4U 1630–47 during part of its 1998 outburst when the 2–10 keV source luminosity decreased from 2.1×10^{38} erg s⁻¹ (for an assumed distance of 10 kpc) by a factor of ~ 7 . The 2–200 keV spectrum can be modeled by a soft multi-temperature disk blackbody and a hard power-law. During four of the observations, there is evidence for deviations from a pure power-law shape $\gtrsim 20$ keV which may be due to reflection. As the outburst decayed a number of spectral trends are evident: (1) the amount of photoelectric absorption decreased, (2) the spectrum became harder (i.e. the power-law index became smaller), (3) the temperature of the disk blackbody decreased and (4) the inferred inner disk radius increased by a factor of ~ 4 . The change in the accretion disk inner radius during the outburst is in contrast to results from other soft X-ray transients. We find that the disk blackbody temperature depends on the inner disk radius roughly as $T \propto r^{-3/4}$. For a standard Shakura-Sunyaev disk model this implies that the inferred mass accretion rate at the inner disk radius did not change appreciably during the part of the outburst observed by *BeppoSAX*.

Key words: X-rays: stars – stars: individual: 4U 1630-47

1. Introduction

4U 1630–47 is an X-ray transient discovered by *Uhuru* (Jones et al. 1976), while the first recorded outburst was detected in 1969 by *Vela 5B* (Priedhorsky 1986). Outbursts occur approximately periodically with intervals ranging from 600–690 days (Jones et al. 1976; Priedhorsky 1986; Kuulkers et al. 1997a). Archival observations are reported in Parmar et al. (1995, 1997b). The 1984 outburst, and its subsequent decay, were relatively well studied by EXOSAT (Parmar et al. 1986). The flux decayed over a period of ~ 100 days from $\sim 2.8 \times 10^{38}$ to 4×10^{36} ergs s⁻¹ (1–50 keV, for an assumed distance of 10 kpc). This distance estimate is based on the high absorption towards the source and

its proximity to the galactic center (Parmar et al. 1986). The relative strength of the soft component decreased by at least a factor of two during the decay and the power-law component became harder as the outburst progressed.

4U 1630–47 is a black hole candidate based on its X-ray spectral and timing behavior (White et al. 1984; Parmar et al. 1986; Kuulkers et al. 1997b). The typical recurrence timescale for black hole candidate outbursts is 10–50 yr (e.g., Parmar et al. 1995), and the more prolific outburst activity of 4U 1630–47 is therefore unusual. No optical counterpart is known, probably due to high reddening and the crowded field (see Parmar et al. 1986). Kuulkers et al. (1997a) predicted that 4U 1630–47 would undergo another outburst near 1998 January 31. It went into outburst on around 1998 February 2, and was detected by the All Sky Monitor (ASM) on-board RXTE (Kuulkers et al. 1998a). The outburst reached a peak 2–12 keV intensity of ~ 460 mCrab on around February 24. During the outburst a radio counterpart was detected by Hjellming & Kuulkers (1998).

We report on five *BeppoSAX* pointed observations performed during the decay of the 1998 outburst. We discuss the 2–200 keV spectrum of 4U 1630–47 and its evolution as the luminosity changed by a factor ~ 7 . In addition, we report on an observation in 1997 March when the source was in quiescence.

2. Observations and analysis

4U 1630–47 was observed five times by *BeppoSAX* during the 1998 February–May outburst (Table 1, see also Fig. 1). Results obtained with the coaligned LECS, MECS, HPGSPC, and PDS instruments are presented. The LECS is sensitive between 0.1–10 keV (Parmar et al. 1997a), the MECS between 2–10 keV (Boella et al. 1997), the HPGSPC between 4–120 keV (Manzo et al. 1997), and the PDS between 15–300 keV (Frontera et al. 1997). The LECS and the MECS are imaging instruments with circular fields of view (FOVs) with diameters of 37' and 56', respectively. The non-imaging HPGSPC consists of a single unit with a collimator that is alternatively rocked on- and off-source to monitor the background spectrum. The non-imaging

Send offprint requests to: T. Oosterbroek (toosterb@astro.estec.esa.nl)

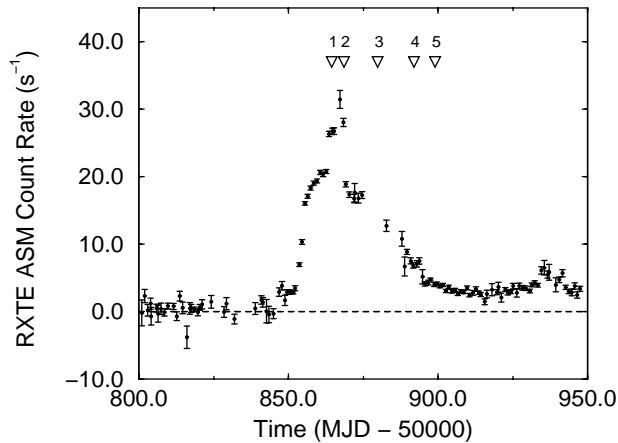


Fig. 1. The RXTE ASM 2–12 keV light curve of the 1998 outburst from 4U 1630–47. The times of the *BeppoSAX* observations are indicated with open triangles. The dashed line indicates the zero level

Table 1. Log of the *BeppoSAX* observations of 4U 1630–47 during its 1998 outburst

Obs	Date (1998)	Start Time (MJD)	Total Time (ks)	MECS Exp. (ks)	MECS Count rate (s ⁻¹)
1	Feb 20	50864.188	42.5	20.0	78.9
2	Feb 24	50868.254	34.1	13.5	75.7
3	Mar 07	50879.517	55.7	29.5	41.8
4	Mar 19	50891.620	48.4	27.7	20.8
5	Mar 26	50898.720	60.0	31.1	11.7

PDS consists of four independent units arranged in pairs each having a separate collimator. Each collimator is operated in a rocking-mode to monitor the background. The HPGSPC and PDS were operated in their nominal modes with a dwell time of 96 s for each on- and off-source position and rocking angles of 210' and 180', respectively. The HPGSPC and PDS have hexagonal FOVs of 78' and 66' full-width at half maximum, respectively.

For the spectral fits only MECS data in the energy range 1.85–10.5 keV and PDS data in the energy range 13–100 keV were used, since – due to the high absorption towards 4U 1630–47 – there is no useful LECS data at lower energies, while the LECS spectrum in the 2–10 keV band is consistent with that from the MECS. Typically, the source is detected with more than 10 σ significance up to 200 keV in the PDS. The PDS spectra were grouped using a logarithmic energy grid and the MECS spectra were grouped such that each energy bin has at least 20 counts. The relative normalization between the instruments was a free parameter to allow for small absolute calibration uncertainties, but the best-fit values are always close to unity.

The HPGSPC data were used to check the spectral shape of the source in the band 10.5–13 keV, which is not covered by the MECS and PDS instruments. The shape obtained from the MECS and PDS is in good agreement with the HPGSPC results. The HPGSPC data were not used in the final fits, because there

are systematic residuals present which may be instrumental in origin. These tend to increase the values of χ^2 (while the best-fit parameters remain unchanged). These residuals may be partly caused by the non-optimal background subtraction (see below) due to the presence of a source in the offset collimator position.

The presence of contaminating sources in the off-source collimator positions of the HPGSPC and the PDS was checked. During the later observations there is clearly a source (probably GX 340+0) in the offset position of the HPGSPC, and in the negative offset position of the PDS. Therefore, data obtained during Earth occultations were used to accumulate background spectra for the HPGSPC, and only the positive offset position was used for the PDS. Due to the different roll-angle of the satellite for each observation, the contribution of this contaminating source is not significant during observations 1 and 2, but in order to obtain a uniform dataset, the same method of background subtraction was used for all five observations. Note that using only one offset spectrum in the background subtraction results in a poorer signal to noise ratio, since the exposure time of the background spectrum is effectively halved.

3. Results

A model consisting of an absorbed multi-temperature disk blackbody (Mitsuda et al. 1984) and an absorbed power-law fits the general broad-band spectral shape reasonably well (Table 2). However, with the exception of the spectra obtained during observation 2, deviations from the best-fit model are present which give rise to formally unacceptable values of χ^2_ν . Fitting the spectra with a combination of absorbed power-law and blackbody models gives similar results. The spectra were next fitted with an absorbed disk blackbody and a cut-off power-law model. This gives some improvement in fit quality, but is still unable to satisfactorily model the deviations, or “wiggles”, in the spectrum which are most prominent around ~ 20 keV (see Fig. 2).

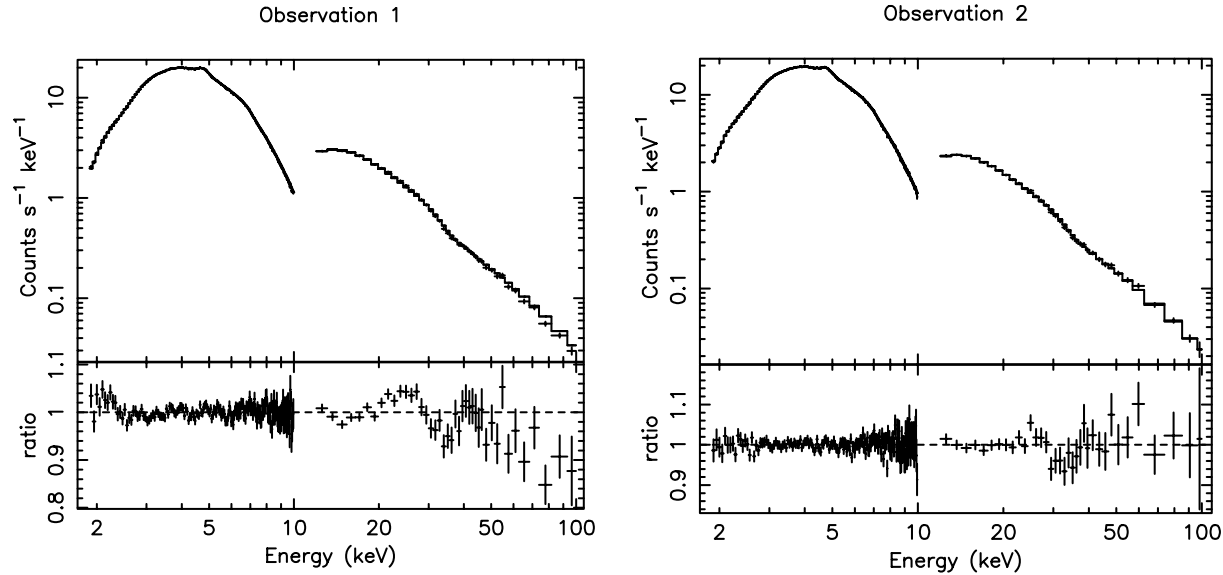
These deviations prompted the use of a model which incorporates reflection such as PEXRIV in XSPEC which models a power-law reflected by ionized material (Magdziarz & Zdziarski 1995). The spectra were fit with the photon index, folding energy, relative reflection, and normalization as free parameters. The best-fit parameters are given in Table 3, with the exception of the folding energy, which was always much larger than highest energy used in the fit. The ionization parameter, ξ , was fixed at 1.0 (corresponding to un-ionized material), since the fits are insensitive to changes in this parameter. The effects of reflection can be seen as deviations from a power-law continuum starting at ~ 10 keV and extending to 30–40 keV in Fig. 3. With this model the overall χ^2_ν is significantly less than with a power-law and disk blackbody model, but individual values are still not always formally acceptable. In comparison with the cutoff power-law model, the values of χ^2_ν are similar for observation 1, while for observations 2–4 the PEXRIV model gives marginally lower values of χ^2_ν (at 90–94% confidence), and for observation 5 the reduction in χ^2_ν is highly significant (>99.9999% confidence). The trends in N_{H} , disk blackbody temperature, and inner disk radius are very similar whichever model is used for the hard

Table 2. The best-fit parameters for a power-law and disk blackbody model. Uncertainties are given at 90% confidence for one parameter of interest. N_{H} is in units of 10^{22} atoms cm^{-2}

Obs	N_{H}	α	Norm ¹ (PL)	T (keV)	Norm ² (Disk BB)	χ^2_{ν}/dof
1	10.33 ± 0.08	2.67 ± 0.01	13.3 ± 0.5	2.21 ± 0.03	13.5 ± 1.3	1.706/246
2	9.88 ± 0.10	2.70 ± 0.2	11.3 ± 0.7	1.96 ± 0.02	27.2 ± 2.0	0.993/246
3	9.00 ± 0.06	2.485 ± 0.01	5.36 ± 0.02	1.13 ± 0.03	111 ± 12	1.631/246
4	8.32 ± 0.08	2.30 ± 0.02	1.10 ± 0.08	1.020 ± 0.015	218 ± 17	1.177/246
5	8.13 ± 0.10	2.28 ± 0.03	0.75 ± 0.05	0.86 ± 0.02	263 ± 30	1.561/246

¹ Photon flux at 1 keV² $(R_{\text{in}}/D_{10})^2 \cos \theta$, where R_{in} is the inner disk radius, D_{10} the distance in units of 10 kpc and θ the disk inclination angle**Table 3.** The best-fit parameters for a PEXRIV and disk blackbody model. All uncertainties are obtained with $\Delta\chi^2 = 2.706$ (90% interval for one parameter of interest). N_{H} is in units of 10^{22} atoms cm^{-2} . L is the 2–10 keV unabsorbed luminosity in units of 10^{38} erg s^{-1} for an assumed distance of 10 kpc. L_{BB}/L is the ratio of luminosity in the disk blackbody compared to the total in the 2–10 keV energy range

Obs	N_{H}	α	Norm ¹ (PEXRIV)	Relative reflection ²	T (keV)	Norm ¹ (Disk BB)	L	L_{BB}/L	χ^2_{ν}/dof
1	$10.03^{+0.21}_{-0.10}$	$2.56^{+0.12}_{-0.04}$	$10.9^{+2.0}_{-0.7}$	<0.19	$2.10^{+0.10}_{-0.03}$	$17.9^{+1.8}_{-3.1}$	2.08	0.29	1.414/244
2	$9.88^{+0.05}_{-0.11}$	2.70 ± 0.01	11.3 ± 0.4	<0.06	$1.96^{+0.02}_{-0.01}$	27.2 ± 2.2	2.00	0.34	1.002/244
3	$9.03^{+0.06}_{-0.11}$	$2.50^{+0.02}_{-0.05}$	$5.51^{+0.20}_{-0.55}$	0.07 ± 0.05	1.13 ± 0.03	$111.0^{+13.5}_{-9.5}$	1.05	0.22	1.608/244
4	$8.39^{+0.05}_{-0.10}$	$2.35^{+0.03}_{-0.05}$	$1.22^{+0.07}_{-0.13}$	$0.18^{+0.08}_{-0.11}$	$1.01^{+0.02}_{-0.01}$	225 ± 17	0.47	0.56	1.151/244
5	8.23 ± 0.16	$2.37^{+0.07}_{-0.12}$	0.79 ± 0.15	$0.69^{+0.23}_{-0.19}$	0.85 ± 0.02	282^{+40}_{-31}	0.27	0.47	1.112/244

¹ Units are the same as in Table 2² Constrained to be positive**Fig. 2.** A comparison of MECS and PDS spectra with strong (*left*, obs. 1) and weak (*right*, obs. 2) “wiggles” at higher energies. The fit model is an absorbed power-law and disk blackbody

component (see e.g. Tables 2 and 3). Therefore the conclusions in Sect. 4 with regard to the derived disk blackbody parameters do not depend on the assumed hard-component model.

Tables 2 and 3 reveal that the temperature of the disk blackbody decreased and the inferred inner disk radius increased as the outburst progressed (see also Fig. 4). To investigate whether

these changes could be artefacts of the fitting procedure, the correlations between the disk blackbody normalization (proportional to the square of the inner disk radius) and the power-law slope and disk blackbody temperature were investigated. Large changes are apparent in these quantities and a (very) strong correlation between parameters could give rise to an apparent

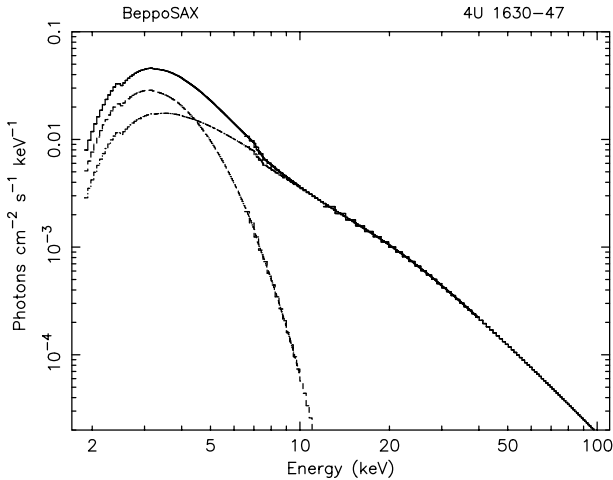


Fig. 3. The photon spectrum of 4U 1630–47 obtained during observation 5 with the MECS, HPGSPC, and PDS instruments. The disk blackbody and power-law-like PEXRIV components are shown separately

change in the inner disk radius (which should then not be interpreted in a physical way). In order to check that this is not the case, contour-plots corresponding to large changes in χ^2 ($\Delta\chi^2=10, 20$) were produced. The confidence contours do not overlap for the different observations since the differences between the obtained parameters are an order of magnitude larger than the size of the confidence contours for these already large χ^2 differences. This analysis reveals that the observed changes are *much* larger than can be explained as due to correlations between fit parameters. The observed changes in the spectral parameters therefore reflect physical changes.

Power spectra of 4U 1630–47 were searched for any distinctive features such as quasi-periodic oscillations. None were found. However, the quality of the power spectra is rather poor (a much better analysis can be done with e.g. RXTE data) and so a more detailed timing analysis was not attempted.

During the *BeppoSAX* observation of 4U 1630–47 in its quiescent state (on 1997 March 26–27), 4U 1630–47 was not detected. However, due to the presence of a number of nearby sources and the relatively poor LECS and MECS spatial resolution, it is difficult to separate the contributions from nearby faint sources. The 3σ upper limit to the MECS count rate is $1.2 \times 10^{-3} \text{ s}^{-1}$. This translates into an upper limit on the 2–10 keV unabsorbed flux of $1.9 \times 10^{33} \text{ ergs s}^{-1}$, for an assumed distance of 10 kpc, a photon index of 2.1, and an N_{H} of $8 \times 10^{22} \text{ atoms cm}^{-2}$ (close to lowest value obtained). This photon index is the value obtained for the black hole candidate GS 2023+338 in quiescence by Narayan et al. (1997). The corresponding value for the unabsorbed 2–10 keV flux for an N_{H} of $2.0 \times 10^{22} \text{ atoms cm}^{-2}$ (the galactic value; Dickey & Lockman 1990) is $1.0 \times 10^{33} \text{ ergs s}^{-1}$. This upper limit is similar to previous limits for the flux of 4U 1630–47 in quiescence (see Parmar et al. 1997b).

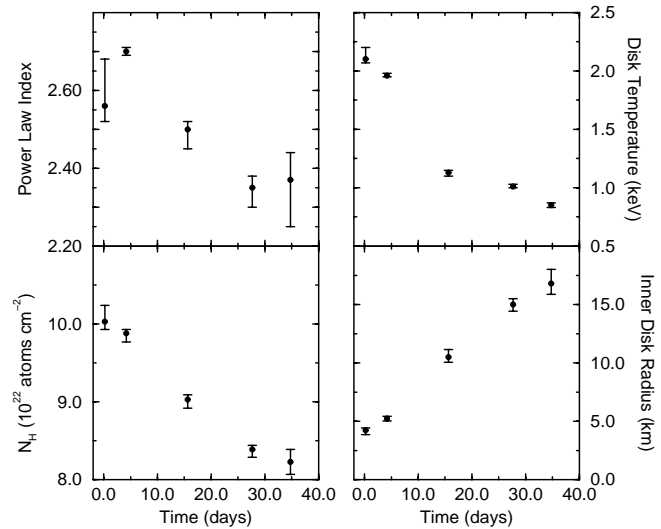


Fig. 4. The changes as a function of time (in days) in the best fit parameters (see Table 3). The uncertainties correspond to 90% confidence intervals. The inner disk radii were obtained assuming a distance of 10 kpc and $\theta = 0^\circ$

4. Discussion

The *BeppoSAX* observations of 4U 1630–47 during its 1998 outburst reveal a decreasing N_{H} , a hardening of a power-law like component, a decreasing disk blackbody temperature, and an increasing inferred inner disk radius (Fig. 4). These first two changes were also observed during the 1986 outburst of 4U 1630–47 by Parmar et al. (1986), and in other X-ray transients (e.g. GS 2023+338; Oosterbroek et al. 1997). The change in N_{H} may suggest that the initial outburst onset is a rather dramatic event, which leaves significant amounts of material around the compact object, which later on is either accreted, or expelled from the system.

The inner disk radius (which has been interpreted as the radius of the innermost stable orbit around a black hole; Ebisawa 1991) increased by a factor of 4 (Fig. 4) during the part of the outburst observed by *BeppoSAX*. Therefore it is clearly not related (at least in a simple way) to the innermost stable orbit. It is interesting to note that a similar phenomenon, as seen in GRS 1915+105 by Belloni et al. (1997), may be evident here: the inner part of the accretion disk changes its state such that it does not contribute to the X-ray flux. However, in GRS 1915+105 this occurs on a much shorter time scale of seconds to minutes. The fact that the best-fit temperature at the inner disk radius decreased during the outburst supports this interpretation - it is just the result of the change in effective inner disk radius. The relation between the best-fit inner disk radii and temperature is shown in Fig. 5. Comparing this to the theoretical temperature profile of a standard Shakura-Sunyaev disk ($T_{\text{s}} \propto r^{-3/4}$, where T_{s} is the surface temperature and r the radius), shows a qualitative agreement. We note that this relation is, strictly speaking, only valid for radii much larger than the inner disk radius. Since the mass accretion rate, $\dot{M} = 8\pi R_{\text{in}}^3 \sigma T^4 / 3GM$ this implies that \dot{M} is approximately constant during the part of the outburst ob-

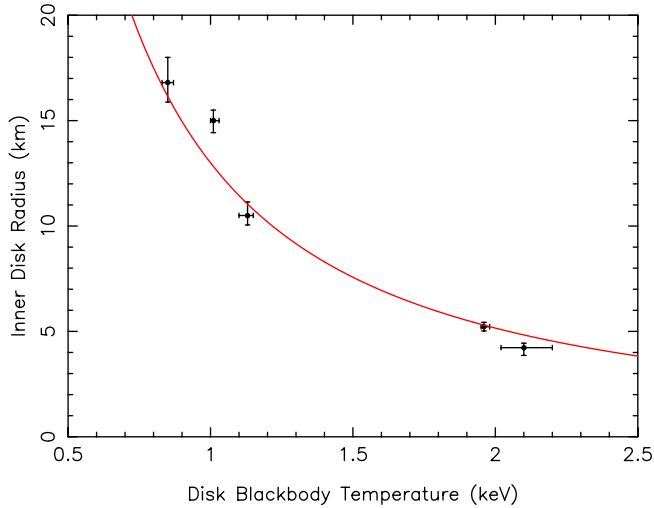


Fig. 5. The relation between the inner disk temperature and the best-fit inner disk radius. The inner disk radii were obtained assuming a distance of 10 kpc and $\theta = 0^\circ$. Points are obtained (in time) from right to left. The solid line represents the theoretical prediction for a standard Shakura-Sunyaev disk model (which is only valid for $r \gg R_{\text{in}}$)

served by *BeppoSAX* (if the contribution from the non-thermal component is excluded), and that the inner part of the accretion disk progressively changed its state to produce the observed spectral changes.

This behavior is quite different from outbursts of the transients GS 1124–68, GRO J1655–40 and GS 2000+25 and from the persistent source LMC X-3 observed by *Ginga* and RXTE. In those sources the best-fit inferred inner disk radii remain approximately constant during the entire outburst (GS 2000+25), or until the late stages ($\gtrsim 150$ days) of the outburst (see Tanaka & Lewin 1995; Ebisawa et al. 1994; Sobczak et al. 1998). This difference is unlikely to be caused by the broad energy coverage of *BeppoSAX*, which allows the underlying power-law(-like) spectrum to be well constrained, since the *Ginga* and RXTE energy ranges extend far beyond where the disk blackbody contributes to the flux. Another difference with respect to the above sources is that their disk blackbody temperatures are $\lesssim 1$ keV, compared to ~ 2 keV with 4U 1630–47 near the peak of the outburst. A similar high temperature was observed in GRS 1915+105 (Belloni et al. 1997). We speculate that the difference in spectral properties may be related to the difference in outburst recurrence intervals between 4U 1630–47 (1.6 yrs) and the other soft X-ray transients which have typical recurrence intervals $\gtrsim 25$ yrs. This may suggest that a different mechanism is responsible for the outbursts in 4U 1630–47, which also gives rise to a different behavior during the outburst. The fact that the inner part of the accretion disk disappears slowly (and smoothly) suggests that the matter accretes into the black hole (as opposed to the sudden phase transition observed in GRS 1915+105). This, in turn, may cause a drop in \dot{M} at the inner edge, which is needed to cause the end of an outburst in irradiated disks (see King & Ritter 1998).

The increase in the best fit inner disk radius is compatible with the model of Esin et al. (1997) who assume that accretion takes place through a Shakura-Sunyaev disk beyond some truncation radius, but within this radius the flow jumps to the advective solution. They model the change from a high to a low state as an increase in the radius where the character of the flow changes. The observed increase in best-fit inner disk radius may therefore simply reflect the outward expansion of the radius where optically thick material is present as the outburst evolved. We note that the best-fit values for the inner disk radius are lower than the value (3 Schwarzschild radii, the innermost marginally stable orbit) for the high state in the Esin et al. (1997) model. However, we have assumed that the disk is viewed face-on (an inclination angle of 0°), while there are indications that the inclination is in the range $60\text{--}75^\circ$ (Kuulkers et al. 1998b). In addition, the distance to the source is uncertain. These factors may result in larger values for the “real” inner disk radius. Życki et al. (1998) also find much smaller values for the inner disk radius from their modeling of the spectra of GS 1124–68, compared to the values predicted in Esin et al. (1997).

We note that the changing inferred inner disk radius has implications for the method applied by Zhang et al. (1997) to determine black hole spin. They calculate the general relativistic effects of black hole rotation on the inner disk regions, which allows the obtained disk blackbody temperatures and inner disk radii to be interpreted in terms of the spin of the black hole. Our results suggest that other processes also affect the spectrum (since a change of black hole spin can be excluded on a time scale of ~ 40 days), which cautions against interpreting spectral properties in terms of black hole parameters alone.

The nature of the hard component in 4U 1630–47 is unclear. Although a reflection model provides the lowest overall χ^2_ν , this does not necessarily mean that significant reflection is occurring in the system. The largest reduction in χ^2_ν using the PEXRIV model compared to a power-law is obtained when the fitted relative reflection is high, which *does* mean that the deviations from a power-law, to first order, can be modeled with a reflection component. However, the values of χ^2_ν are not always formally acceptable, which suggests that, although the PEXRIV model gives a better overall fit than a power-law or a cutoff power-law, the detailed modeling of the reflected component is unsatisfactory. We note that the fits to the EXOSAT spectra also gave formally unacceptable χ^2 values, although Parmar et al. (1986) used a different model consisting of a Wien-like soft component and a power-law. It appears that the spectrum of 4U 1630–47 is complex and contains features which cannot be currently modeled in a realistic way.

The amount of reflection in the PEXRIV model (see Table 3) increased, compared to the underlying continuum, as the outburst decayed. However, there is no obvious correlation between the amount of relative reflection and the normalizations of the disk blackbody and power-law, as modeled with the PEXRIV model, suggesting that any reflected component is neither constant nor directly related to the strengths of either spectral component. The weakness of the “wiggles” during observation 2 coincided with the peak of the outburst, as can be seen from

the RXTE ASM light curve (Fig. 1). This may be coincidence, or it could be that the continuum becomes “smoother” near the maximum of the outburst as a rule. We note that the residuals in the $\sim 4\text{--}7$ keV range become significantly less if a narrow Gaussian component is added, suggesting the presence of a weak (~ 30 eV equivalent width) iron line (obs. 3). However, the residuals are at the 2–3% level, comparable to the systematic uncertainties. In comparison with Active Galactic Nuclei where reflection components and associated iron fluorescence lines have been detected from a number of systems (e.g., Pounds et al. 1990), the lack of intense ($\gtrsim 100$ eV equivalent width) iron emission from 4U 1630–47 is surprising, if reflection is important in this system. However, we note that during a Broad Band X-ray Telescope observation of the blackhole candidate Cyg X-1 by Marshall et al. (1993) also showed evidence for reflection by material surrounding the central source, but only a narrow line at 6.4 keV with an equivalent width of 13 ± 11 eV was possibly detected.

Acknowledgements. The *BeppoSAX* satellite is a joint Italian–Dutch programme. T. Oosterbroek acknowledges an ESA Fellowship. We thank the staff of the *BeppoSAX* Science Data Center for their support and the RXTE/ASM teams at MIT and at NASA’s GSFC for providing quick-look results.

References

- Belloni T., Méndez M., King A.R., van der Klis M., van Paradijs J., 1997, *ApJ* 479, L145
- Boella G., Chiappetti L., Conti G., et al., 1997, *A&AS* 122, 327
- Dickey J.M., Lockman F.J., 1990, *ARA&A* 28, 215
- Ebisawa K., 1991, Ph.D. Thesis, ISAS, University of Tokyo
- Ebisawa K., Ogawa M., Aoki T., et al., 1994, *PASJ* 46, 375
- Esin A.A., McClintock J.E., Narayan R., 1997, *ApJ* 489, 865
- Frontera F., Costa E., Dal Fiume D., et al., 1997, *A&AS* 122, 357
- Hjellming R.M., Kuulkers E., 1998, *IAU Circ.* 6827
- Jones C., Forman W., Tananbaum H., Turner M.J.L., 1976, *ApJ* 210, L9
- King A.R., Ritter H., 1998, *MNRAS* 293, L42
- Kuulkers E., Parmar A.N., Kitamoto S., Cominsky L.R., Sood R.K., 1997a, *MNRAS* 291, 81
- Kuulkers E., van der Klis M., Parmar A.N., 1997b, *ApJ* 474, L47
- Kuulkers E., Dieters S., McCollough M., et al., 1998a, *IAU Circ.* 6822
- Kuulkers E., Wijnands R., Belloni T., et al., 1998b, *ApJ* 494, 753
- Magdziarz P., Zdziarski A.A., 1995, *MNRAS* 273, 837
- Manzo G., Giarusso S., Santangelo A., et al., 1997, *A&AS* 122, 341
- Marshall F.E., Mushotzky R.F., Petre R., Serlemitsos P.J., 1993, *ApJ* 419, 301
- Mitsuda K., Inoue H., Koyama K., et al., 1984, *PASJ* 36, 741
- Narayan R., Barret D., McClintock J.E., 1997, *ApJ* 482, 448
- Oosterbroek T., van der Klis M., van Paradijs J., et al., 1997, *A&A* 321, 776
- Parmar A.N., Stella L., White N.E., 1986, *ApJ* 304, 664
- Parmar A.N., Angelini L., White N.E., 1995, *ApJ* 452, L129
- Parmar A.N., Martin D.D.E., Bavdaz M., et al., 1997a, *A&AS* 122, 309
- Parmar A.N., Williams O.R., Kuulkers E., Angelini L., White N.E., 1997b, *A&A* 319, 855
- Pounds K.A., Nandra K.P., Stewart G.C., George I.M., Fabian A.C., 1990, *Nat* 344, 132
- Priedhorsky W.C., 1986, *AP&SS* 126, 89
- Sobczak G.J., McClintock J.E., Remillard R.A., Bailyn C.D., Orosz J.A., 1998, *ApJ* submitted (astro-ph/9809195)
- Tanaka Y., Lewin W.H.G., 1995, In: Lewin W.H.G., van Paradijs J., van den Heuvel E.P.J. (eds.) *X-ray Binaries*. Cambridge Univ. Press, Cambridge, 126
- White N.E., Kaluzienski J.L., Swank J.H., 1984, In: Woosley S.E. (ed.) *High Energy Transients in Astrophysics*. Proc AIP Conf. 115, AIP, New York, 31
- Zhang S.N., Cui W., Chen W., 1997, *ApJ* 482, L155
- Życki P.T., Done C., Smith D.A., 1998, *ApJ* 496, L25